Applied Surface Science Advances 18 (2023) 100497

Contents lists available at ScienceDirect

Applied Surface Science Advances

journal homepage: www.sciencedirect.com/journal/applied-surface-science-advances

Effect of oxygen plasma-treatment on surface functional groups, wettability, and nanotopography features of medically relevant polymers with various crystallinities

Paulina Chytrosz-Wrobel [a], Monika Golda-Cepa [a,*], Ewa Stodolak-Zych [b], Jakub Rysz [c], Andrzej Kotarba [a]

[a] Faculty of Chemistry, Jagiellonian University in Krakow, Gronostajowa 2, Krakow 30-387, Poland,
[b] Department of Biomaterials and Composites, Faculty of Materials Science and Ceramics, AGH University of Krakow, Al. Mickiewicza 30, Krakow 30-059, Poland
[c] Faculty of Physics Astronomy and Applied Computer Science, Jagiellonian University, Lojasiewicza 11, Krakow 30-348, Poland

ARTICLE INFO

Keywords:
Atomic force microscopy
Surface modification
Plasma treatment

ABSTRACT

The surface properties of polymeric biomaterials play a crucial role in their biocompatibility and performance. This study explores the application of cold oxygen plasma treatment as a versatile technique for surface modification of polymeric materials with different degrees of crystallinity: crystalline high-density polyethylene (HDPE), crystalline-amorphous poly(chloro-paraxylylene) (parylene C), and amorphous aromatic polyether-based polyurethane (PU). The investigations focus on the generation of surface functional groups and hydrophilicity, as well as nanotopography. X-ray photoelectron spectroscopy (XPS) analysis confirmed the generation of oxygen-containing functional groups, resulting in controlled wettability (water contact angle), while atomic force microscopy (AFM) showed topography modifications in the nanoscale. At the same time, it was revealed that oxygen plasma treatment did not affect the bulk properties (confirmed by TG and XRD). The effects of the same plasma treatment conditions varied significantly among the different polymers studied, depending on their crystallinity. This was discussed in terms of the preferential etching of amorphous regions in the polymeric structures. The findings emphasize the advantages of oxygen plasma treatment for tailoring the surface properties of polymeric biomaterials, highlighting its significance for biomedical applications.

1. Introduction

Polymers are the most widely explored and promising type of materials for applications in medical devices, implants, stents, etc. [1–3]. The structural and property range of monomers renders them fundamental for tissue engineering technology. From a chemical perspective, the design of polymeric materials is limited by creativity, time, and resources [3]. The global market for medical polymers is projected to exceed $24 billion by 2024, indicating their commercial significance [4]. The trend is also visible in the scientific papers published in the last decade (2013–2022), with the keywords "polymer" and "biomaterial" appearing in over 120k publications. Among them, > 35,000, > 20,000, and > 800 were devoted to polyethylene (PE), polyurethanes (PUs), and parylenes, respectively.

Owing to their carbon-based chemistry, polymers are more compatible with human tissues than inorganic materials [5]. Their widespread use in biomedical applications stems from their vast variety of structures, tunable properties (physical, chemical, surface), and low fabrication costs. A wide range of applications include coatings (e.g., anti-corrosive) [6], drug delivery systems (hydrogels, micelles, or polymer-drug conjugates) [7,8], and bulk implants (e.g., bone pins and screws, catheters, and membranes) [9–11].

One of the most important properties of polymeric materials is their degree of crystallization. Crystallinity in polymers is more difficult to define than in other classes of materials (e.g., inorganic materials), because of their complicated morphology [12]. Polymers typically exhibit two types of long polymeric chains: arranged (lamellae) or amorphous. Arranged lamellar structures are called crystalline, although crystalline polymers are rarely encountered (usually with up to 80–90 % of crystallinity). In a polymer structure, there are always amorphous regions that originate from the incompatibility of the long chains. The amorphous regions are composed of unsystematically coiled

* Corresponding author.
E-mail address: mm.golda@uj.edu.pl (M. Golda-Cepa).

https://doi.org/10.1016/j.apsadv.2023.100497
Received 12 July 2023; Received in revised form 2 November 2023; Accepted 8 November 2023
Available online 15 November 2023

and entangled chains. The third possibility is a semi-crystalline structure, in which both crystalline and amorphous domains are observed. Such a structure is desirable in polymeric biomaterials, as it combines the strength of the crystalline domain, and the flexibility of the amorphous regions [13–15].

To utilize the full potential of polymers in bio-applications, surface modification technologies are required to improve their performance. Overall, these include wet and dry methods, that are subdivided in synthetic chemistry [16], solutions of modifying reagents [17], and applying reactive chemical compound vapors [18]. In general, the wet chemistry approach is labor-intensive, and requires numerous steps and solvents. Therefore, dry methods, such as low-pressure gas plasma, seem to be efficient alternatives with a shorter functionalization time, easier scalability, and implementation of green chemistry principles (zero-waste processes) [19]. Thus, plasma technology has become an important and versatile surface-modification technique. Plasma, the fourth state of matter, comprises a mixture of free electrons, positively charged ions, neutral atoms and/or molecules, free radicals, and ultraviolet (UV) photons. By fitting the modification parameters (feed gas type, feed gas pressure, generator power, and treatment time), the level of surface functionalization can be controlled and limited to a depth of only several nanometers without altering the properties of the bulk material [20,21]. Plasma is widely used for various applications in biotechnology, such as polymerization, coating deposition, cleaning, sterilization, and functionalization [20]. By using oxygen as a gas source for plasma, surface oxygen-containing groups can be incorporated in a controllable and reproducible manner, thereby improving the biocompatibility of the material [22].

So far, the plasma treatment was successfully used to functionalize several medically relevant polymers to create bioactive surfaces with adsorbed proteins [23], cellular response [24], and tissue integration [25]. Although the plasma modification of polymers is a widely used technology, systematic research on its influence on polymers with different crystallinity is still missing. The ratio of crystalline and amorphous regions seems to be crucial in terms of modification efficiency as even when the same plasma parameters are applied, different surface properties can be obtained.

To fulfill this knowledge gap, we investigate the influence of oxygen plasma treatment on the surface morphology and structure of three polymers (Fig. 1) with different degrees of crystallinity: crystalline high-density polyethylene (HDPE), semi-crystalline poly(chloro-paraxylylene) (parylene C), and amorphous aromatic polyether-based polyurethane (PU). We examine the changes in the topographical properties before and after plasma treatment via water contact angle measurements, XPS, and AFM observations. Parallelly, the structural changes are determined by XRD and TG measurements.

2. Experimental

2.1. Materials

Three polymeric foils with different degrees of crystallinity were prepared: high-density polyethylene crystalline (Polypak), parylene C semi-crystalline (ParaTech Coating), and amorphous aromatic polyether-based polyurethane (American Polyfilm, Inc.). To remove contaminants, the polymer surfaces were washed with 2-propanol (Avantor) and dried at room temperature (22 °C).

2.2. Plasma modification

Functionalization of the polymeric surfaces was performed using a plasma generator (FEMTO system, Diener Electronics, Germany). Samples of 20 × 20 mm were prepared, and oxygen (SIAD Poland 6.0 pure 99,9999 %) was used as the feed gas to functionalize the materials with oxygen–containing groups and generate the nanotopography features. The oxygen base pressure in the chamber was 0.14 mbar, with a fixed generator power of 50 W and a modification time of 1 min.

2.3. Methods

X-ray Diffraction (XRD) was used to determine the crystallinity of the polymeric samples. The measurements were performed with a Rigaku MiniFlex diffractometer with the Bragg-Brentano focusing geometry, and Cu Kα X-ray source (λ = 1.5406 Å) operating at 10 mA and 10 kV. The measurements were performed in the 2θ range of 3 to 65° with a step size of 0.02°. The samples were in the form of thin polymeric films (6–80 μm) of the macroscopic surface area of 1.5 × 1.5 cm^2.

Thermogravimetric analysis (TG) was used to study the bulk properties of the polymeric samples. The measurements were carried out using a Mettler Toledo 851e apparatus, in a temperature range of 30–600 °C with a heating rate of 10°/min and under Ar flow of 50 mL/min. For comparison, the measured mass loss of samples (~ 5–7 mg) was normalized to 100 %.

Tensile mechanical strength testing of film specimens was carried out using a Zwick Roell Z2.5 testing machine. Plasma-modified and reference polymeric films were tested in uniaxial tension. The tested working area (jaw distance) was 20 mm. The tested materials had widths in the range of 7–8 mm and their thicknesses were 7 μm (Parylene C), 80 μm (PU) and 6 μm (HDPE), respectively. The test speed was 20 mm/min with a material tensile speed of 1 mm/min in the range in which the modulus was determined. At least 8 measurements were taken for each of the reference and plasma-modified materials. The obtained results were analyzed in terms of the mean Young modulus value (x) and the standard deviation (s).

Water contact angle (WCA) analysis was used to probe the hydrophobic/hydrophilic properties of the polymeric samples. Changes in the wettability of the polymers were monitored using a Surftens Universal (OEG GmbH) goniometer with the Surftens 4.3 software. The 1.5 μL drops of double-distilled water and diiodomethane (Merck) were placed on the polymeric surfaces and the static contact angle was measured (at least 10 drops, random sample spots). After ten measurements at different positions on each sample, the average value was calculated. The surface free energy (SFE) was determined using the Owens–Wendt method [26]. The method is based on two liquid measurements (polar-water and nonpolar-diiodomethane). The surface tension and polar and dispersion components of SFE for these liquids are well-known and described in the literature.

$$\gamma_s = \gamma_s^d + \gamma_s^p$$

$$\left(\gamma_s^d\right)^{1/2} = \frac{\gamma_d(cos\theta_d + 1) - \sqrt{(\gamma_d^p/\gamma_w^p)}\gamma_w(cos\theta_w + 1)}{2\left(\sqrt{\gamma_d^d} - \sqrt{\gamma_d^p\left(\gamma_w^d/\gamma_w^p\right)}\right)}$$

$$\left(\gamma_s^p\right)^{1/2} = \frac{\gamma_w(cos\theta_w + 1) - 2\sqrt{\gamma_s^d\gamma_w^d}}{2\sqrt{\gamma_w^p}}$$

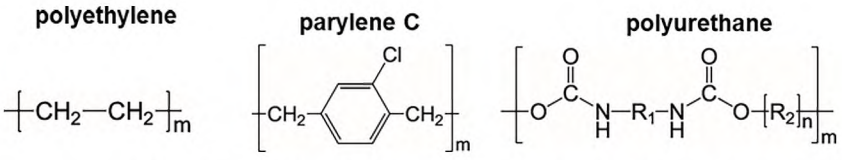

Fig. 1. The chemical formulas for high-density polyethylene, parylene C, and polyurethane (R_1 is the isocyanate, R_2 is the polyol).

where, γ_s is the SFE, γ_s^d dispersive component of surface energy of the investigated material, γ_s^p polar component of SFE of the investigated material, γ_d total free energy of diiodomethane (50.8 mN/m), γ_d^p and γ_d^d polar (2.3 mN/m) and dispersive (48.5 mN/m) constants of total free energy of diiodomethane, respectively, γ_w total free energy of water (72.8 mN/m), γ_w^p and γ_w^d polar (51.0 mN/m), and dispersive (21.8 mN/m), (50.8 mN/m), constants of total free energy of water, respectively, θ_d and θ_w contact angle of diiodomethane and water, respectively.

X-ray photoelectron spectroscopy (XPS) was used to examine the changes in the surface composition and identify the surface functional groups on the polymeric samples after plasma treatment. A SES R4000 analyzer (Gammadata Scienta), with a monochromatic Al Kα X-ray source (1486.6 eV) at 250 W (pass energy: 100 eV) in ultrahigh vacuum (10^{-9} mbar) was used for the survey and narrow scans. The acquired XPS spectra were analyzed using the Casa-XPS 2.3.15 software. The spectra were calibrated against the C 1 s peak at 285.0 eV.

Atomic Force Microscopy (AFM) was used to observe changes in the surface morphology of the samples after plasma treatment. Observations were performed using a JPK NanoWizard 4 XP system equipped with an Olympus optical microscope and an active vibration isolation platform (Accurion i4). All the experiments were conducted under air and ambient conditions in an acoustic enclosure. A Bruker scanning probe (TESPG-V2 Si doped with an Sb tip) operating at a resonance frequency of ~320 kHz and a typical spring constant of ~42 N/m was used. The scan area was 5 × 5 μm^2 and the scan frequency range was 0.5–1 Hz. The JPK Data Processing software was used to process the obtained topographic images and roughness (root mean square RMS) calculations. For each investigated polymeric samples the evaluation of surface roughness was performed for five-six randomly selected area locations.

3. Results and discussion

3.1. Bulk properties

Low-pressure plasma can be used to modify the top-surface layer of a material without altering its bulk properties [27]. The process was controlled by the precise adjustment of the working parameters of the plasma generator (power, working gas partial pressure, and time of treatment). To monitor the effect of plasma exposure on the polymeric materials, the samples were characterized using bulk and surface-dedicated techniques. The stability of the polymer structures was investigated using XRD and TG analyses (Fig. 2).

The XRD results for HDPE, indexed in the *Pnam* space group, before (Fig. 2A, blue curve) and after the plasma (Fig. 2A, orange curve) treatment remained unchanged, confirming the stability of the crystalline structure. Both patterns show three maxima at 2θ = 21.3°, 23.7°, and 29.1°, corresponding to the (110), (200), and (210) crystal planes, respectively, which agree well with the literature [28]. The broad peak at 2θ = 19° corresponds to the amorphous parts of HDPE [29].

The diffractograms for parylene C presented in Fig. 2B show a characteristic maximum at 2θ = 13.7°, which can be indexed to the (020) plane in the *P1* space group [30]. The broad maximum at 2θ = 20–40° was assigned to the amorphous domains of this polymer.

The absence of sharp diffraction maxima in the XRD pattern of polyurethane (Fig. 2C) confirms the purely amorphous structure of this polymer. For both samples, broad maxima in the range of 2θ = 10–30° were observed, and their shapes remained unchanged upon oxygen plasma treatment, confirming the stability of the polyurethane-disordered structure. The XRD details (2θ,FWHM, D, d) are provided in Table S1.

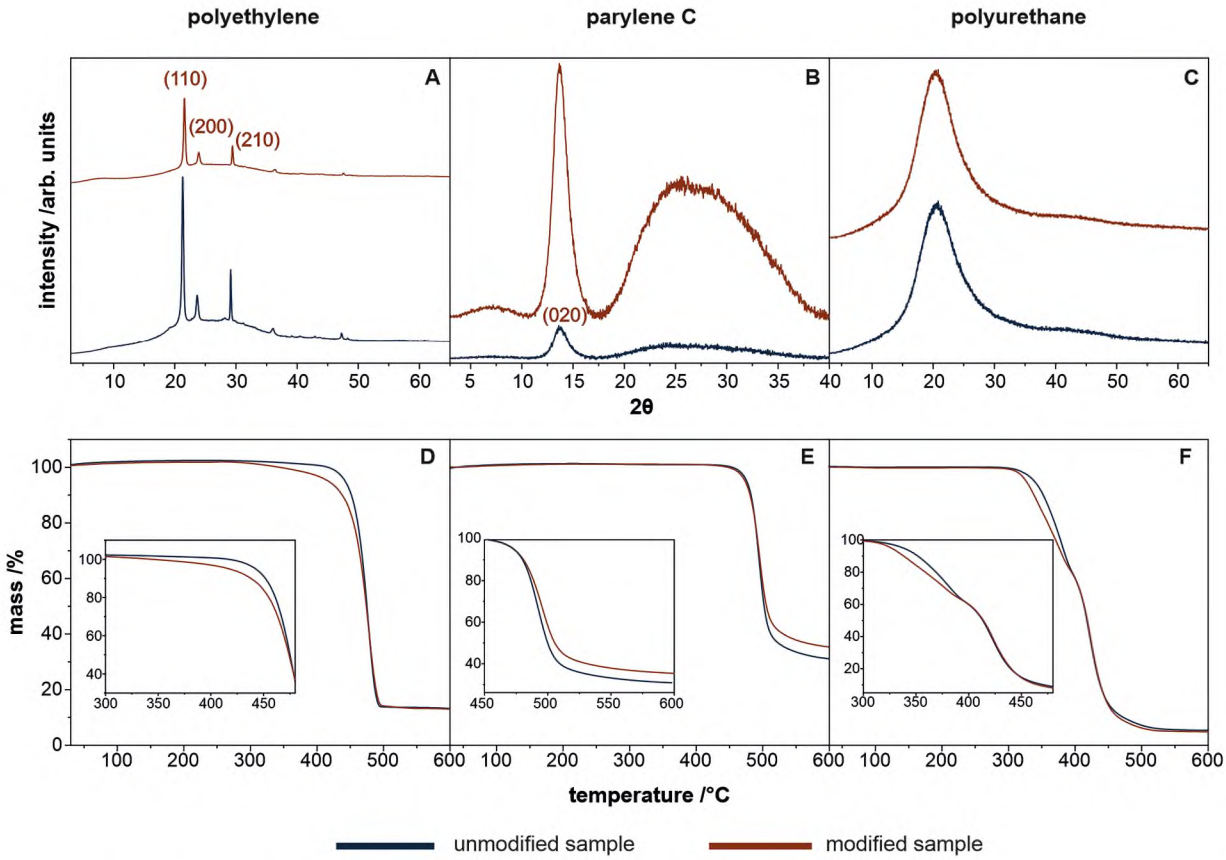

Fig. 2. The diffractograms (A-C) accompanied by the thermogravimetric curves (D-F) for the unmodified (blue lines) and oxygen plasma-modified (1 min, 50 W, 0.14 mbar O_2) polymeric samples (orange lines): high-density polyethylene (A, D), parylene C (B, E) and polyurethane (C, F), respectively. The insets in the lower panel show the region of changes in magnification.

Representative TG profiles for HDPE, parylene C, and polyurethane are presented in Fig. 2 D–F, respectively, along with the insets magnifying the regions of interest for the investigated samples. The highly crystalline HDPE was stable up to 270 °C, and began to gradually degrade when reaching higher temperatures (Fig. 2D). As a consequence of oxygen plasma modification, the observed thermal degradation of HDPE is more rapid in the temperature range of 270–470 °C [31].

The amorphous-crystalline parylene C, built of stable aromatic rings, is highly thermally stable, up to 430 °C, as can be inferred from Fig. 2E. The TG profiles revealed that the oxygen plasma treatment did not appreciably affect the thermal stability. Nevertheless, the weight losses of the modified samples (35 %) were lower than those of the unmodified samples (32 %). These results can be attributed to the enlarged crystallites of the modified parylene C structure, which are more thermally stable and shift the polymer degradation to higher temperatures.

The amorphous polyurethane (Fig. 2F) exhibited the lowest thermal stability among the investigated polymers, and the two–step degradation, which stemmed from the presence of two different types of monomers (isocyanate and polyol) in the polyurethane film, was observed already at 260 °C. The plasma modification accelerates the degradation in the range of 260–400 °C, which results from the preferential cleavage of the C–C bonds present in the soft segments of the polyurethane structure.

The differences in the bulk structure of the polymers are also reflected in their mechanical properties. Taking into account the specific properties of polymeric materials, the Young modulus values were used as the most relevant descriptor of the effect of plasma treatment. Indeed, this parameter varies in a large range from 24 ± 3 MPa (for polyurethane), passing through 257 ± 104 MPa (for HDPE) to the highest observed value of 968 ± 73 MPa (for parylene C). The corresponding values for modified polyurethane, HDPE, and parylene C equals 17 ± 1, 308 ± 105, and 897 ± 114 MPa, respectively. The force curves obtained from the mechanical tests for all the investigated polymers can be found in the Supporting Information (Fig. S1). Considering all the data obtained from the measurements using structure-sensitive methods XRD, TG, and mechanical tests it can be thus concluded, that the oxygen plasma modification does not lead to significant changes in the material's bulk. However, it should be underlined that this conclusion is valid only for mild plasma conditions with the parameters optimized for surface functionalization only.

3.2. Surface functional groups

Plasma-induced changes in surface chemistry (i.e., the generation of surface functional groups) are reflected in host biological responses to biomaterials, and their controlled tailoring is of utmost importance [32, 33]. Thus, the surfaces of the investigated samples were characterized by XPS to evaluate the surface state (composition and oxidation level) before and after the oxygen plasma treatment. The survey spectra are presented in Fig. 3 for unmodified and oxygen plasma-modified samples of high-density polyethylene (A), parylene C (B), and polyurethane (C), respectively. The wide-scan XPS spectra of the investigated polymeric materials display only the main constituent elements: oxygen O 1s at 533 eV and carbon C 1s at 285 eV for HDPE; oxygen O 1s at 533 eV, carbon C 1s at 285 eV and chlorine Cl 2s at 270 eV for parylene C; and carbon C 1s at 285 eV, nitrogen N 1s at 399 eV, and oxygen O 1s at 533

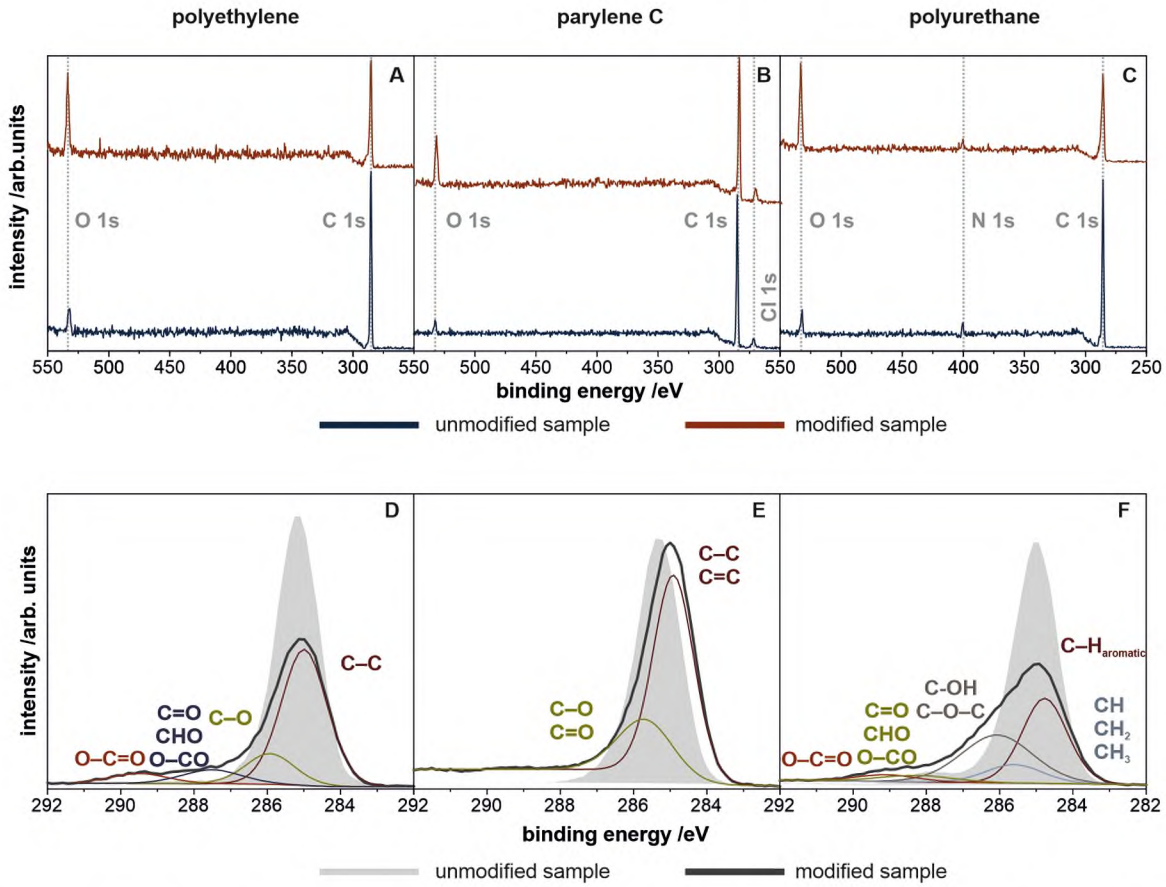

Fig. 3. The XPS survey scans (A–C) together with the narrow scans for C1s (D-F) of the unmodified (blue lines for upper panel, gray shadowing for lower panel) and oxygen plasma modified (1 min, 50 W, 0.14 mbar O_2) polymeric samples (orange lines for upper panel, black lines for lower panel): high-density polyethylene (A, D), parylene C (B, E) and polyurethane (C, F), respectively. The details about FWHM and atomic percentages for carbon components for oxygen plasma-modified polymeric surfaces are supplied in Table S2.

eV for polyurethane. The detailed atomic percentage data are summarized in Table S3. As expected, for all studied polymeric samples, a significant increase in the O 1s peak signal after plasma modification was observed.

The estimated value of the incorporated oxygen was approximately 15 %; consequently, the C 1 s signal intensity decreased by 15 %.

XPS allows not only the identification of the surface elemental composition but also the characterization and identification of the chemical nature of the generated functional groups. Therefore, a detailed analysis of the C 1s peaks of the high-resolution spectra for the HDPE, parylene C, and polyurethane samples is presented in Fig. 3 D–F, respectively. For all the investigated polymeric samples, several components were fitted and attributed to specific carbon chemical oxidation states. As expected, broadening of the carbon peak upon oxidation was observed for all three polymers investigated: HDPE (D), parylene C (E), and polyurethane (F). In particular, for HDPE two new components can be distinguished in the region of 286.4–289.3 eV, corresponding to oxygen-containing groups (C=O, CHO, O–CO, and O–C=O) present at the polymeric surface [34,35]. For parylene C, the widening of the component at 285.7 eV can be attributed to the C–O and C=O bonds [36]. For polyurethane, two new peaks appear in the range of 286.4–289.3 eV, assigned to the oxidized surface carbon to C–OH, C–O–C, and O–C=O groups [37,38].

The XPS results for the three polymers confirmed the surface oxidation of these materials. Although the same plasma process parameters were applied, the modification resulted in different amounts of surface oxygen groups and their different chemical natures.

3.3. *Surface topography*

The importance of the surface topography of biomaterials must be considered as strongly relevant, as surface roughness plays an important role in bacterial and cell adhesion [39,40].

The influence of oxygen plasma treatment on the surface topography of the polymers was monitored using AFM. For representative results, the surface areas of 5 × 5 μm^2 of all the investigated samples were examined in several randomly selected locations. The AFM images of the unmodified and oxygen plasma-modified samples are presented in Fig. 4A, B, together with the corresponding cross-sections, showing the detailed topography profiles in the z-direction.

It can be seen that the surface of unmodified polyethylene (Fig. 4 A1) is fairly smooth and wavy, with a small number of peaks and valleys (which results from the technological manufacturing process). After the oxygen plasma treatment, the HDPE surface (Fig. 4 A2) became highly rough, with a large number of nanocorrugations when compared to the unmodified reference. Analysis of the data presented in Fig. 4 A1 and A2 shows a decrease in the R_{RMS} value from 107 to 38 nm. The increase in the number of corrugations was also pronounced in the cross-section of the modified polyethylene. These observations can be attributed to the effect of plasma etching of the polymeric surfaces. After exposure to the oxygen plasma, the HDPE surface becomes rougher as preferential etching of the amorphous residues between the crystal domains occurs. However, it is also possible that some segregation of the crystalline domains on the surface may occur [41].

Examination of the unmodified parylene C surface topography (Fig. 4 B1) revealed a smooth surface with visible scratches (left after the deposition process). After plasma treatment (Fig. 4 B2), morphological

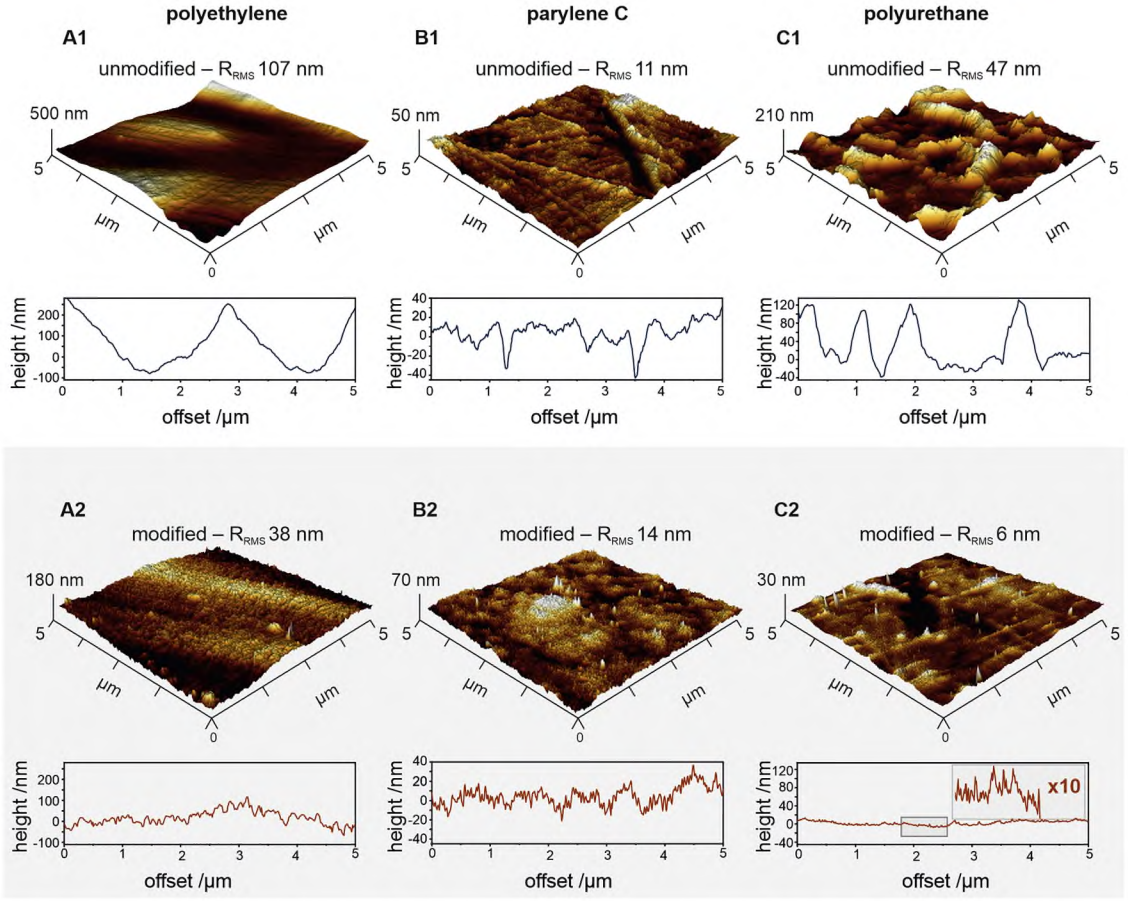

Fig. 4. The 3D representations of AFM images of unmodified (white panel) and oxygen plasma modified (1 min, 50 W, 0.14 mbar O_2) (gray panel) polymeric surfaces for high-density polyethylene (A), parylene C (B) and polyurethane (C), together with the cross-section profiles. For comparison, the R_{RMS} parameter values describing their surface roughness are provided for each AFM image.

changes were visible, and the surface was rough with a large number of nanopeaks and valleys, which was also confirmed in the cross-sectional profile. The image analyses of Fig. 4 B1 and B2 show an increase in the R_{RMS} value from 11 to 14 nm. The plasma modification of parylene C resulted in the generation of nanotopography as a result of the preferential etching of the amorphous regions, thus exposing the crystalline domains on the surface.

The AFM images of the unmodified polyurethane sample (Fig. 4 C1) reveal hills and valleys in the range of 100–300 nm. The sample treated with oxygen plasma presented significant changes in surface morphology, where nanosized pores appeared. More irregularities were observed in the lower range up to 20 nm along the Z-axis. Thus, the surface roughness of the untreated sample was greatly decreased compared to that of the plasma-treated sample (R_{RMS} value from 47 to 6 nm). This was because of the uniform initial etching of the polyurethane surface over time, whereas during the modification process, the soft segments were more susceptible to etching. This also provides space for the reorientation of stable hard segments, which are responsible for the nanoroughness of the resulting surface.

In summary, for all modified samples, numerous peaks and valleys were observed in the topography, indicating that the oxygen plasma treatment strongly affects the surfaces of these polymers, despite the degree of crystallinity. The R_{RMS} of highly crystalline HDPE and amorphous polyurethane decreased, while the R_{RMS} for the crystalline-amorphous parylene C increased.

3.4. Wettability

The XPS, SIMS, and AFM results provide insights into the alteration of both the surface chemistry (presence of oxygen-containing functional groups) and topography (nanoscale corrugations). These changes significantly affect the hydrophilicity of the polymeric surface. Most polymeric biomaterials require the adjustment of their surface properties to stimulate cell adhesion. As water is the most abundant and small molecule that comes into contact with biomaterials in the human body, surface – water interactions are of key importance. One of the common descriptors of material biocompatibility is wettability, which is experimentally quantified using the water contact angle. Thus, the effect of the oxygen plasma on the wettability of the investigated samples was explored, and the results are summarized in Fig. 5. The 1 min plasma treatment resulted in a completely wettable surface for HDPE and parylene C (Fig. 5A and B, respectively). For the amorphous polyurethane, the water contact angle decreased from 100° (unmodified surface) to 20° (modified for 1 min), Fig. 5C. All observed changes in the water contact angle were caused by the generation of polar oxygen functional groups on the polymeric surfaces, which strongly affected the interaction of water with the functionalized surfaces.

In addition to wettability, the surface free energy (SFE) is another important descriptor for characterizing the surface-cell interface of biomaterials. Consequently, changes in the surface free energies were calculated for all the polymeric samples. For the unmodified samples, the greatest contribution to the SFE was from the dispersive component, which varied as 41 mJ/m^2 for parylene C, 38 mJ/m^2 for HDPE, and 28 mJ/m^2 for polyurethane. After exposure to the oxygen plasma, the dispersive component decreased slightly for HDPE and parylene C, whereas the opposite tendency was observed for polyurethane. A dramatic increase in the polar components was observed for the modified surfaces of all the three investigated polymers. After modification with the oxygen plasma, the SFE value stabilized at 70–73 mJ/m^2.

In Fig. 6, the most important results are graphically epitomized to illustrate the effect of the oxygen plasma treatment on the surface morphology of the three polymers with different degrees of crystallinity. Depending on the bulk structure of the polymer, the selectivity of the etching behavior results in the formation of different surface morphologies. HDPE, which is composed of crystalline domains (Fig. 6A) owing to its ordered and dense structure, exhibits a high resistance to plasma etching. Amorphous polyurethane (Fig. 6C), on the other hand, is more susceptible to plasma etching as it is constructed of loosely coiled polymeric chains. However, in this case, the erosion or removal of the polymer material was homogeneous, and the resultant topography was relatively flat. For the crystalline-amorphous parylene C (Fig. 6B), etching occurred preferentially in the amorphous regions, leading to a characteristic surface with nanocorugations of varying densities and depths.

The various observed effects of plasma on the polymer surface have important practical implications, revealing the need for the precise adjustment of etching parameters to obtain the desired surface finish. For the application of these polymers in biomedicine, functional groups [42], wettability [43], and nanotopography [44] are considered critical factors. As shown above, all these properties can be tailored by plasma treatment for a specific biomaterial-tissue interface.

These findings are particularly important in the context of tested polymer applications. The crystallinity of polymeric biomaterials strongly influences their mechanical properties, chemical and wear resistance. Therefore, crystalline structure directly impacts long-lasting performance. Highly crystalline polymers tend to be stiffer, more chemically resistant, and less prone to wear, making them suitable for load-bearing applications and those requiring extended stability. In case of the tested polymers, all of them are medically relevant and used in biomaterials; amorphous polyurethane in short-term (up to three

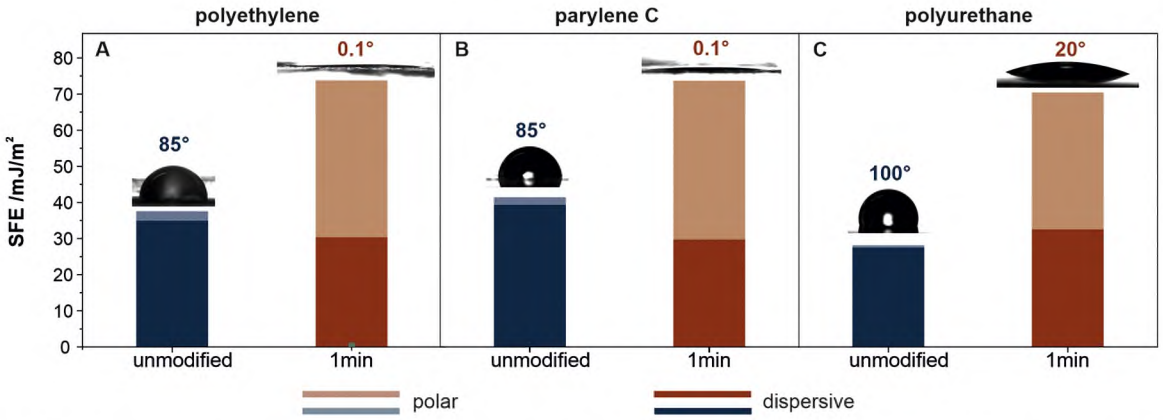

Fig. 5. SFE values for the unmodified (blue bars) and oxygen plasma modified (1 min, 50 W, 0.14 mbar O_2) samples (orange bars) of high-density polyethylene (A), parylene C (B) and polyurethane (C), respectively, together with water contact angle values. The error bars for the calculated SFE values are <5 % and are not shown. The detailed numerical values of the water CA, diiodomethane CA and Surface Free Energy (SFE) together with the corresponding errors can be found in Supporting Information Table S4.

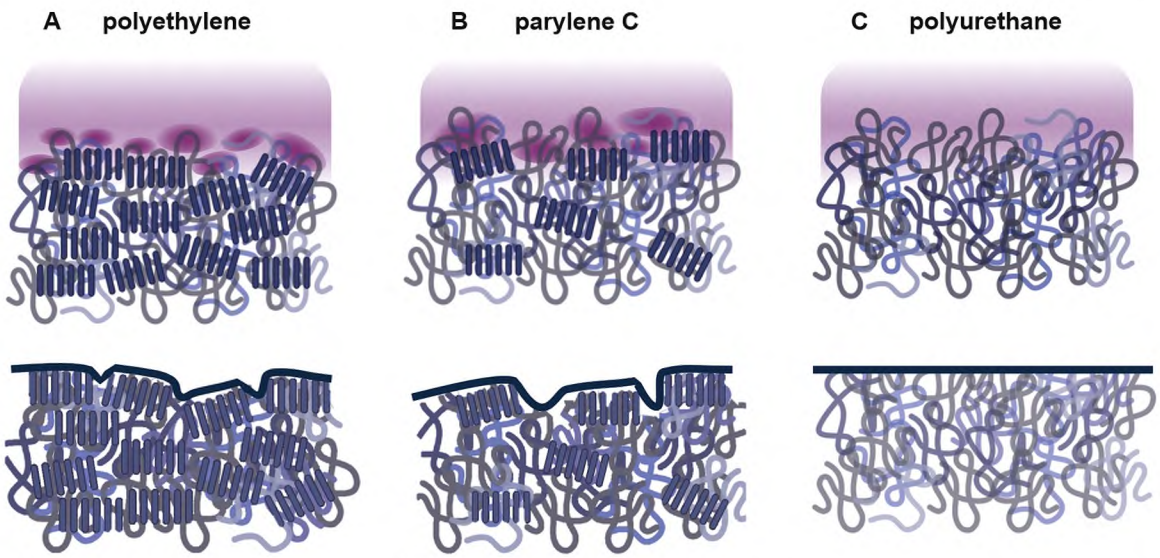

Fig. 6. Schematic representation of polymeric structures with different degrees of crystallinity illustrating various etching mechanisms resulting in different surface morphology of the investigated polymers (lower panel). Darker spots in the upper panel indicate the amorphous regions where preferential etching takes place. The models were built based on the XRD and AFM results for structural and topographic characterization.

months) esophageal stents, semicrystalline parylene C as anti-corrosive coating for long-term metal implants and crystalline polyethylene as the mobile cup in hip endoprosthesis. The performance of all these materials can be improved by controlled surface modification.

4. Conclusions

In this study, cold oxygen plasma treatment was proven to be an effective technique for modifying the surface properties of polymeric materials (HDPE, parylene C, and polyurethane) without affecting their bulk properties. Changes in crucial properties such as the chemical nature of the generated functional groups, wettability, and nano-topography of the polymeric materials were studied. Although the stability of the polymer structures was confirmed by XRD, TG and mechanical tests, the surface chemistry (generation of oxygen-containing functional groups) was revealed by XPS analysis. The modification of the surface topography at the nanoscale was monitored by AFM. The effects of the same plasma treatment conditions varied significantly among the different polymers studied, depending on their crystallinity. This was explained in terms of preferential etching of the amorphous regions and exposure of the crystalline domains on the surface. Overall, the findings of this study highlight the potential of oxygen plasma treatment for tailoring the surface properties of polymeric biomaterials, emphasizing the importance of the individual optimization of plasma parameters depending on the crystalline-amorphous nature of the polymer.

Declaration of Competing Interest

The authors declare that they have no known competing financial interests or personal relationships that could have appeared to influence the work reported in this paper.

Data availability

Data will be made available on request.

Acknowledgment

This work was supported by the National Science Centre, Poland, under grant no. DEC-2019/35/D/ST5/03107.

Supplementary materials

Supplementary material associated with this article can be found, in the online version, at doi:10.1016/j.apsadv.2023.100497.

References

[1] M. Mir, M.N. Ali, A. Barakullah, A. Gulzar, M. Arshad, S. Fatima, M. Asad, Synthetic polymeric biomaterials for wound healing: a review, Prog. Biomater. 7 (1) (2018) 1–21, https://doi.org/10.1007/S40204-018-0083-4.
[2] A.J.T. Teo, A. Mishra, I. Park, Y.J. Kim, W.T. Park, Y.J. Yoon, Polymeric biomaterials for medical implants and devices, ACS Biomater. Sci. Eng. 2 (2016) 454–472, https://doi.org/10.1021/acsbiomaterials.5b00429.
[3] M.L. Becker, J.A. Burdick, Introduction: polymeric biomaterials, Chem. Rev. 121 (18) (2021), https://doi.org/10.1021/acs.chemrev.1c00354.
[4] Medical Polymers Market, https://www.gminsights.com/industry-analysis/medical-polymers-market, Report I: GMI1126, (Published Dec 2022, Accessed November 09, 2023).
[5] M.F. Maitz, Applications of synthetic polymers in clinical medicine, Biosurf. Biotribol. 1 (3) (2015) 161–176, https://doi.org/10.1016/j.bsbt.2015.08.002.
[6] M. Golda-Cepa, A. Chorylek, P. Chytrosz, M. Brzychczy-Wloch, J. Jaworska, J. Kasperczyk, M. Hakkarainen, K. Engvall, A. Kotarba, Multifunctional PLGA/parylene C coating for implant materials: an integral approach for biointerface optimization, ACS Appl. Mater. Interfaces 8 (34) (2016) 22093–22105, https://doi.org/10.1021/acsami.6b08025.
[7] S. Sur, A. Rathore, V. Dave, K.R. Reddy, R.S. Chouhan, V. Sadhu, Recent developments in functionalized polymer nanoparticles for efficient drug delivery system, Nano Struct. Nano Objects 20 (2019), 100397, https://doi.org/10.1016/j.nanoso.2019.100397.
[8] Y.K. Sung, S.W. Kim, Recent advances in polymeric drug delivery systems, Biomater. Res. 24 (1) (2020) 1–12, https://doi.org/10.1186/s40824-020-00190-7, 2020.
[9] M. Barde, M. Davis, S. Rangari, H.C. Mendis, L. De La Fuente, M.L. Auad, Development of antimicrobial-loaded polyurethane films for drug-eluting catheters, J. Appl. Polym. Sci. 135 (27) (2018) 46467, https://doi.org/10.1002/app.46467.
[10] R. Agarwal, A.J. García, Biomaterial strategies for engineering implants for enhanced osseointegration and bone repair, Adv. Drug. Deliv. Rev. 94 (2015) 53–62, https://doi.org/10.1016/j.addr.2015.03.013.
[11] M.A.A. Ansari, A.A. Golebiowska, M. Dash, P. Kumar, P.K. Jain, S.P. Nukavarapu, S. Ramakrishna, H.S. Nanda, Engineering biomaterials to 3D-print scaffolds for bone regeneration: practical and theoretical consideration, Biomater. Sci. 10 (11) (2022) 2789–2816, https://doi.org/10.1039/d2bm00035k.
[12] C.B. Crawford, B. Quinn, Physiochemical properties and degradation. Microplastic Pollutants, Elsevier Science, 2017, pp. 57–100, https://doi.org/10.1016/b978-0-12-809406-8.00004-9.
[13] K. Balani, V. Verma, A. Agarwal, R. Narayan, Physical, thermal, and mechanical properties of polymers. Biosurfaces, Wiley, 2015, pp. 329–344, https://doi.org/10.1002/9781118950623.app1.

[14] A. Popelka, S. Zavahir, S. Habib, Morphology analysis. Polymer Science and Innovative Applications: Materials, Techniques, and Future Developments, Elsevier, 2020, pp. 21–68, https://doi.org/10.1016/b978-0-12-816808-0.00002-0.
[15] C. De Rosa, F. Auriemma, Crystal structures of polymers. Handbook of Polymer Crystallization, Wiley, 2013, pp. 31–72, https://doi.org/10.1002/9781118541838.ch2.
[16] E. Biazar, M. Kamalvand, F. Avani, Recent advances in surface modification of biopolymeric nanofibrous scaffolds, Int. J. Polym. Mater. 71 (2022) 493–512, https://doi.org/10.1080/00914037.2020.1857383.
[17] D.H. Ga, C.M. Lim, Y. Jang, T. Il Son, D.K. Han, Y.K. Joung, Surface-modifying effect of zwitterionic polyurethane oligomers complexed with metal ions on blood compatibility, Tissue Eng. Regen. Med. 19 (2022) 35–47, https://doi.org/10.1007/s13770-021-00400-w.
[18] T.G. Vladkova, D.N. Gospodinova, Plasma based approaches for deposition and grafting of antimicrobial agents to polymer surfaces. Urinary Stents: current State and Future Perspectives, Springer, 2022, pp. 273–289, https://doi.org/10.1007/978-3-031-04484-7.
[19] K. Lau, B. Akhavan, M.S. Lord, M.M. Bilek, J. Rnjak-Kovacina, Dry surface treatments of silk biomaterials and their utility in biomedical applications, ACS Biomater. Sci. Eng. 6 (10) (2020) 5431–5452, https://doi.org/10.1021/acsbiomaterials.0c00888.
[20] E. Akdoğan, H.T. Şirin, Plasma surface modification strategies for the preparation of antibacterial biomaterials: a review of the recent literature, Mater. Sci. Eng. C 131 (2021), 112474, https://doi.org/10.1016/j.msec.2021.112474.
[21] F. Khelifa, S. Ershov, Y. Habibi, R. Snyders, P. Dubois, Free-radical-induced grafting from plasma polymer surfaces, Chem. Rev. 116 (6) (2016) 3975–4005, https://doi.org/10.1021/acs.chemrev.5b00634.
[22] S. Yoshida, K. Hagiwara, T. Hasebe, A. Hotta, Surface modification of polymers by plasma treatments for the enhancement of biocompatibility and controlled drug release, Surf. Coat. Technol. 233 (2013) 99–107, https://doi.org/10.1016/j.surfcoat.2013.02.042.
[23] L.V. Tapia-Lopez, M.A. Luna-Velasco, E.K. Beaven, A.S. Conejo-Dávila, M. Nurunnabi, J.S. Castro, RGD peptide-functionalized polyether ether ketone surface improves biocompatibility and cell response, ACS Biomater. Sci. Eng. 9 (2023) 5270–5278, https://doi.org/10.1021/acsbiomaterials.3c00232.
[24] N. Al-Azzam, A. Alazzam, Micropatterning of cells via adjusting surface wettability using plasma treatment and graphene oxide deposition, PLoS One 17 (2022), e0269914, https://doi.org/10.1371/journal.pone.0269914.
[25] M. Mohseni Garakani, P. Ahangar, S. Watson, B. Nisol, M.R. Wertheimer, D. H. Rosenzweig, A. Ajji, A novel 3D co-culture platform for integrating tissue interfaces for tumor growth, migration and therapeutic sensitivity: "PP-3D-S, Biomater. Adv. 134 (2022), 112566, https://doi.org/10.1016/j.msec.2021.112566.
[26] M. Golda-Cepa, M. Brzychczy-Wloch, K. Engvall, N. Aminlashgari, M. Hakkarainen, A. Kotarba, Microbiological investigations of oxygen plasma treated parylene C surfaces for metal implant coating, Mater. Sci. Eng. C 52 (2015) 273–281, https://doi.org/10.1016/j.msec.2015.03.060.
[27] T. Jacobs, R. Morent, N. De Geyter, P. Dubruel, C. Leys, Plasma surface modification of biomedical polymers: influence on cell-material interaction, Plasma Chem. Plasma Process. 32 (2012) 1039–1073, https://doi.org/10.1007/s11090-012-9394-8.
[28] A.A. Alsaygh, J. Al-Hamidi, D.A. Fares, I.M. Al-Najjar, V.L. Kuznetsov, Characterization of polyethylene synthesized by zirconium single site catalysts, Appl. Petrochem. Res. 4 (2014) 79–84, https://doi.org/10.1007/s13203-014-0053-2.
[29] M.M.H. Shirazi, M. Khajouei-Nezhad, S.M. Zebarjad, R. Ebrahimi, Evolution of the crystalline and amorphous phases of high-density polyethylene subjected to equal-channel angular pressing, Polym. Bull. 77 (2020) 1681–1694, https://doi.org/10.1007/s00289-019-02827-7.
[30] B.J. Kim, B. Chen, M. Gupta, E. Meng, Formation of three-dimensional Parylene C structures via thermoforming, J. Micromech. Microeng. 24 (6) (2014), 065003, https://doi.org/10.1088/0960-1317/24/6/065003.
[31] N. Médard, J.C. Soutif, F. Poncin-Epaillard, Characterization of CO2 plasma-treated polyethylene surface bearing carboxylic groups, Surf. Coat. Technol. 160 (2002) 197–205, https://doi.org/10.1016/S0257-8972(02)00407-3.
[32] C. Ma, L. Wang, A. Nikiforov, Y. Onyshchenko, P. Cools, K.(Ken) Ostrikov, N. De Geyter, R. Morent, Atmospheric-pressure plasma assisted engineering of polymer surfaces: from high hydrophobicity to superhydrophilicity, Appl. Surf. Sci. 535 (2021), 147032, https://doi.org/10.1016/j.apsusc.2020.147032.
[33] H. Amani, H. Arzaghi, M. Bayandori, A.S. Dezfuli, H. Pazoki-Toroudi, A. Shafiee, L. Moradi, Controlling cell behavior through the design of biomaterial surfaces: a focus on surface modification techniques, Adv. Mater. Interfaces 6 (13) (2019), 1900572, https://doi.org/10.1002/admi.201900572.
[34] A. Van Deynse, P. Cools, C. Leys, R. Morent, N. De Geyter, Surface modification of polyethylene in an argon atmospheric pressure plasma jet, Surf. Coat. Technol. 276 (2015) 384–390, https://doi.org/10.1016/j.surfcoat.2015.06.041.
[35] E. Gonzalez, R.F. Hicks, Surface analysis of polymers treated by remote atmospheric pressure plasma, Langmuir 26 (2010) 3710–3719, https://doi.org/10.1021/la9032018.
[36] M. Gołda, M. Brzychczy-Włoch, M. Faryna, K. Engvall, A. Kotarba, Oxygen plasma functionalization of parylene C coating for implants surface: nanotopography and active sites for drug anchoring, Mater. Sci. Eng. C. 33 (2013) 4221–4227, https://doi.org/10.1016/j.msec.2013.06.014.
[37] I. Mrsic, T. Bäuerle, S. Ulitzsch, G. Lorenz, K. Rebner, A. Kandelbauer, T. Chassé, Oxygen plasma surface treatment of polymer films—Pellethane 55DE and EPR-g-VTMS, Appl. Surf. Sci. 536 (2021), 147782, https://doi.org/10.1016/j.apsusc.2020.147782.
[38] J. Friedrich, The Plasma Chemistry of Polymer Surfaces: Advanced Techniques for Surface Design, Wiley, 2012, https://doi.org/10.1002/9783527648009.
[39] V.R. Kearns, R.J. McMurray, M.J. Dalby, Biomaterial surface topography to control cellular response: technologies, cell behaviour and biomedical applications. Surface Modification of Biomaterials: Methods Analysis and Applications, Woodhead Publising, 2011, pp. 169–201, https://doi.org/10.1533/9780857090768.1.169.
[40] S. Khalid, A. Gao, G. Wang, P.K. Chu, H. Wang, Tuning surface topographies on biomaterials to control bacterial infection, Biomater. Sci. 8 (24) (2020) 6840–6857, https://doi.org/10.1039/d0bm00845a.
[41] M. Golda-Cepa, K. Engvall, A. Kotarba, Development of crystalline–amorphous parylene C structure in micro- and nano-range towards enhanced biocompatibility: the importance of oxygen plasma treatment time, RSC Adv. 5 (60) (2015) 48816–48821, https://doi.org/10.1039/c5ra06366c.
[42] N.R. Richbourg, N.A. Peppas, V.I. Sikavitsas, Tuning the biomimetic behavior of scaffolds for regenerative medicine through surface modifications, J. Tissue Eng. Regen. Med. 13 (8) (2019) 1275–1293, https://doi.org/10.1002/term.2859.
[43] M.M. Gentleman, E. Gentleman, The role of surface free energy in osteoblast–biomaterial interactions, Int. Mater. Rev. 59 (8) (2014) 417–429, https://doi.org/10.1179/1743280414y.0000000038.
[44] K. Harawaza, B. Cousins, P. Roach, A. Fernandez, Modification of the surface nanotopography of implant devices: a translational perspective, Mater. Today Bio 12 (2021), 100152, https://doi.org/10.1016/j.mtbio.2021.100152.